in vivo *31*: 1131-1137 (2017)
doi:10.21873/invivo.11179

FT-IR Spectroscopy Study in Early Diagnosis of Skin Cancer

MARIA KYRIAKIDOU[1], JANE ANASTASSOPOULOU[1], ARISTEIDIS TSAKIRIS[1,2], MARIA KOUI[1] and THEOPHILE THEOPHANIDES[1]

[1]*Laboratory of Radiation Chemistry & Biospectroscopy, Chemical Engineering School, National Technical University of Athens, Athens, Greece;*
[2]*Department of Plastic and Reconstructive Surgery, 401 General Military Hospital of Athens, Athens, Greece*

Abstract. *Background/Aim: Mid-infrared spectroscopy (4000-500 cm^{-1}) was used to analyze the spectral changes and differences of the characteristic absorption bands of the skin components due to cancer development for early clinical diagnosis. Materials and Methods: Human biopsies from basal cell carcinoma, malignant melanoma, and nevus were used, while normal skin tissue served as a control. Results: The high quality of Fourier-transform infrared (FT-IR) spectra showed that upon cancer development the intensity of the absorption band at approximately 3062 cm^{-1} was increased, indicating that most of the proteins had the configuration of amide B and the β-sheet protein structure predominated. The stretching vibration bands of vCH_2 in the region 2950-2850 cm^{-1} were increased in melanoma and nevus, while were less pronounced in basal cell carcinoma due to the increased lipophilic environment. In addition, the intensity of a new band at 1744 cm^{-1}, which is assigned to aldehyde, was increased in melanoma and nevus and appeared as a shoulder in the spectra of normal skin. The absorption band of amide I at 1650 cm^{-1} was split into two bands, at 1650 cm^{-1} and 1633 cm^{-1}, due to the presence of both α-helix and random coil protein conformations for melanoma and nevus. This was confirmed from the amide II band at 1550 cm^{-1}, which shifted to lower frequencies at 1536 cm^{-1} and 1540 cm^{-1} for basal cell carcinoma and melanoma, respectively, indicating a damage of the native structure of proteins. The bands at 841 and 815 cm^{-1}, which are assigned to B-DNA and Z-DNA, respectively, indicated that only the bands of the cancerous Z-DNA form are pronounced in melanoma, while in BCC both the characteristic bands of B-DNA and Z-DNA forms are found. Conclusion: It is proposed that the bands described above could be used as "diagnostic marker" bands for DNA forms, in the diagnosis of skin cancer.*

Correspondence to: Theophile Theophanides, Chemical Engineering School, Radiation Chemistry & Biospectroscopy, National Technical University of Athens, Zografou Campus, 15780 Athens, Greece. Tel: +30 6936993712, e-mail: theo.theophanides@gmail.com

Key Words: Skin cancer, basal cell carcinoma (BCC), melanoma (MM), nevous (NEV), infrared spectroscopy, diagnostic bands.

Skin melanoma and non-melanoma cancer rates increase every year globally. Skin is a highly metabolic tissue and acts as a protective barrier between the body and the harmful environmental factors. Sun UV and ionizing radiation are responsible for sun burns, premature aging, and skin carcinogenesis. The mechanisms of skin carcinogenesis have been extensively studied (1-6). Basal cell carcinoma (BCC), squamous-cell carcinoma (SCC), and skin melanoma (MM) are the three main types of skin cancer (7). BCC is the most common non-melanoma skin cancer, grows slowly, invades locally, and is rarely metastatic (7, 8). SCC is more likely to spread and is characterized by erythematous lesions (6). Finally, melanoma is the most aggressive skin cancer.

The clinical diagnosis of skin cancer includes histological data, size and shape of skin lesions. Fourier Transform-Infrared (FT-IR) spectroscopy provides multidimensional information about the components of a tissue, and can be used as a tool for the non-invasive characterization and identification of the molecular features of various cancer types. The IR spectra consist the "fingerprint" of any material, including tumor tissues and are very sensitive to structural changes of the biological molecules that are formed due to biochemical and metabolic processes that occur during cancer development (9-12). The mid-IR spectra (4000-400 cm^{-1}) of normal and malignant tissues indicated that FT-IR spectroscopy could be useful in the diagnosis of skin cancers (9-12). FT-IR spectroscopy today is a rapid and easy-to-use method. Infrared spectra of excellent quality can be obtained from skin cancer tissues immediately after resection surgery, without any pre-preparation of the samples. This is a major advantage of Attenuated Total Reflection (ATR)-FT-IR spectroscopy for the histopathological assessment of skin cancers. However, the depths achieved by IR spectroscopy cannot exceed 20 μm

(13). In the present work we used ATR-FT-IR spectroscopy to evaluate the spectral differences between healthy cells and BCC, melanoma, and nevus *in vitro*, in order to identify characteristic "marker bands" that can be used for diagnostic purposes.

Materials and Methods

Patients. For the *in vitro* study, biopsies were received from 4 patients with BCC on the head (8 specimens), 2 patients with MM on the back (8 specimens), and 1 patient with nevus (NEV) on the neck (2 specimens). Normal skin tissue from the healthy region adjacent to the extracted damaged skin was used as a control. The size of the biopsies did not allow separation of the epidermal layers. Parts of each biopsy were sent for histopathological analysis to confirm the type and stage of cancer. Tissues were fixed in 10% neutral-buffered formalin immediately after surgical excision. Paraffin was not used for tissue fixation, since we have observed that when using solvents such as hexane and DMSO to remove paraffin from the samples, the lipophilic soluble products and aggregates produced during cancer development are not detected in the spectra (data not shown). Biopsies were obtained from non-pretreated patients during surgery, according to the Greek ethical rules, with the permission of the Scientific Board of the 401 Army General Hospital in Athens.

ATR-FT-IR spectroscopy. Spectra were recorded with an ATR-FT-IR Nicolet 6700 thermo-scientific spectroscope as previously described (14). The ATR-FT-IR technique does not require homogenized samples, thus we were able to obtain spectra from different parts within each tissue specimen. In order to minimize the signal-to-noise ratio, each spectrum consisted of 120 co-added spectra at a spectral resolution of 4 cm^{-1}. The OMNIC 7.3 software program was used for data analysis.

Results and Discussion

FT-IR spectra (4000-400 cm^{-1}) of normal healthy tissue (N), BCC, MM and NEV biopsies are shown in Figure 1. The spectra of BCC, MM, and NEV show variations in intensities and frequency shifts in wavenumbers of the absorption bands, in comparison to the healthy tissues.

The absorption bands of the stretching vibrations of *v*OH and *v*NH groups of glycosaminoglycans, proteins, and collagen of the skin, as well as the stretching vibration bands of the water molecules in the cells appear in the spectral region between 4000 and 3000 cm^{-1} as previously reported (12-18). In Figure 1, the broad band at approximately 3484 cm^{-1} in the spectra of N and NEV is assigned to the stretching vibration of *v*OH groups of water molecules, and to the *v*OH of polysaccharides of the hyaluronic acid (HA). This band is decreased in the cases of BCC and MM due to the skin dehydration and to the HA chain degradation. The intense band at 3290 cm^{-1} is assigned to the stretching vibration of *v*NH groups of proteins and it shows that the protein formulation is in the form of Amide A, as previously shown (18, 19). Deconvolution analysis in this region showed that this *v*NH band consisted of 5 absorption bands (spectra not included here), which correspond to stretching vibrations of *v*NH groups of proteins and *v*OH of glycosaminoglycans, which interact with each other and form various strengths of hydrogen bonds.

The band at approximately 3062 cm^{-1} indicates that most of the proteins have the configuration of amide B. In the case of amide B, the β-sheet protein structure predominates (19). This means that the effect of the NH group of the peptide bond –NHCO- is stronger than C=O, unlike in amide A, where the effect of C=O in the peptide bond is stronger. The coexistence of both A and B protein conformations illustrates the prevalence of different hydrogen bonds that hold the protein strands together (14, 19). As it is known, the hydrogen bond is important in stabilizing the protein helix and any change implies that the physiological environment has changed. We have found that these changes are very important and constitute a basic criterion in order to characterize the disease and its progression (10-18).

The bands in the spectral region between 3000 cm^{-1} to 2870 cm^{-1} (Figure 1) are assigned to the symmetric and antisymmetric stretching vibrations of methyl ($v_{as}CH_3$, v_sCH_3) and to methylene ($v_{as}CH_2$, v_sCH_2) groups of lipids, proteins, and glycosides (9-12, 15). A considerable increase of the intensity of these bands is observed in the spectra of MM and NEV, and less in BCC spectra, indicating that the environment of the membrane has changed and the surrounding medium has become more lipophilic (15). Deconvolution of BCC, MM, and NEV spectra showed the production of a new band at 2892 cm^{-1} in this region, which is assigned to the presence of a branched alkyl chain. The formation of branched alkyl chain indicated that, through the metabolic pathways of the disease, free alkyl radicals were produced, which interacted with each other to give final stable dimer products. Moreover, increase of the intensities of the symmetric absorptions of $vsCH_2$ groups confirmed the higher order configuration of the lipid membranes, indicating the production of amyloids, due to cancer formation (11, 12, 16).

The spectral region 1800-700 cm^{-1} contains information about the secondary structure of proteins (Figure 1). The new band at 1744 cm^{-1} in N and BCC spectra appears as a shoulder, but in MM and NEV has much higher intensity and is assigned to aldehyde group (-CHO), which is formed as a result of lipid peroxidation (16, 17). The high intensity band near 1650 cm^{-1} is assigned to *v*C=O vibrations of the amide I of the peptide bond (-NHCO-) of proteins (16-19). For MM and NEV samples, this band, upon deconvolution, was split into two bands at 1650 cm^{-1} and 1633 cm^{-1}, due to the presence of both α-helix and random coil protein conformations. The next intense band at about 1550 cm^{-1} is assigned to amide II of the proteins β-turns and it suggests that the collagen has α-helix configuration. This band also was

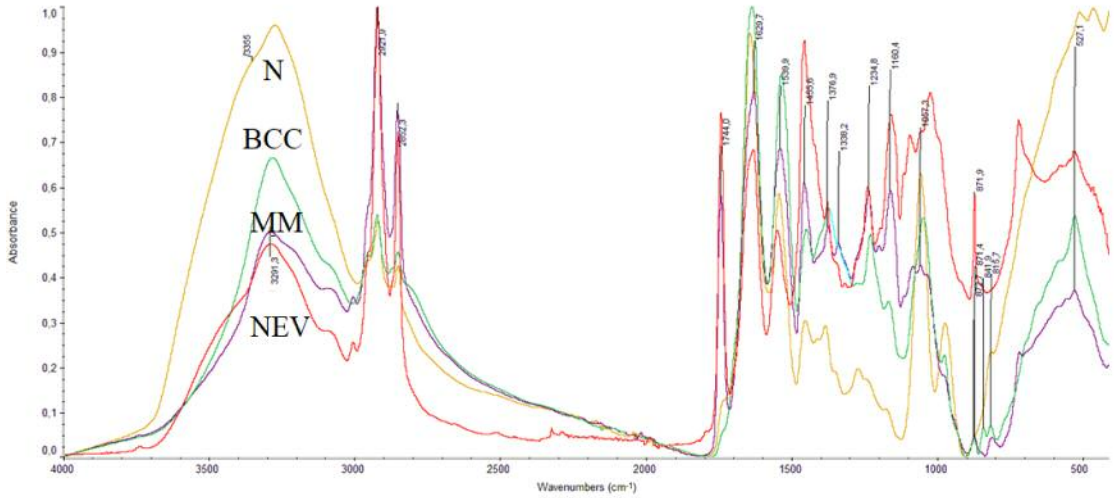

Figure 1. *FT-IR spectra of skin tissues: normal healthy tissue (N), basal cell carcinoma (BCC), melanoma (MM) and nevus (NEV), in the region 4000-400 cm^{-1}.*

shifted to lower frequencies, from 1544 cm^{-1} for healthy cells to 1536 cm-1 for BCC, 1540 cm^{-1} for MM, and 1549 cm^{-1} for NEV, indicating a damage of the native structure of proteins. Noticeable changes were also observed in the spectral region of 1250-1000 cm^{-1}, including the absorptions of the -PO_2- and -C-O-C- group vibrations, where an oxygen atom is linked to two carbon atoms of the sugar moiety of glycosaminoglycans together with the exocyclic C-O-C inter-molecule groups (19). The bands near 1150-1165 cm^{-1} are attributed to -C-O-C bonds of the sugar ring of HA and to sugar ring of DNA (20, 21). The band at 1056 cm^{-1} is assigned to exocyclic -C-O-C- (oxygen bridge). The absorption bands of the C-C and C-OH appear at 1160 cm^{-1}. As it is shown in Figure 1, this band increased in intensity in the spectra of BCC, MM, and NEV, indicating that there was substantial reduction in the amount of hydrogen-bonded C-OH groups of cellular proteins, as well as an accumulation of carbohydrates as a result of glycosylation during the cancer progression. This band was also observed in the cancer regions of breast and colon, and metastatic bone cancers (10, 12, 22).

Figure 2 shows the FT-IR spectra of normal healthy tissue (N), basal call carcinoma (BCC), melanoma (MM) and nevus (NEV) specimens. Region 900-800 cm^{-1} reveals information on the configuration of the sugar-phospahte groups of DNA backbone. The absorption bands at 841 cm^{-1} and 815 cm^{-1} are assigned to sugar-phosphate vibrations of backbone strands of DNA and correspond to B-DNA and Z-DNA, respectively (23, 24). In the case of MM, only the cancerous Z-DNA conformation was observed, while in BCC both B-DNA and Z-DNA forms were found. In the normal tissue the band of B-DNA was masked from other absorptions. The high intensity band at 871 cm^{-1} is attributed to tyrosine amino acid (25, 26).

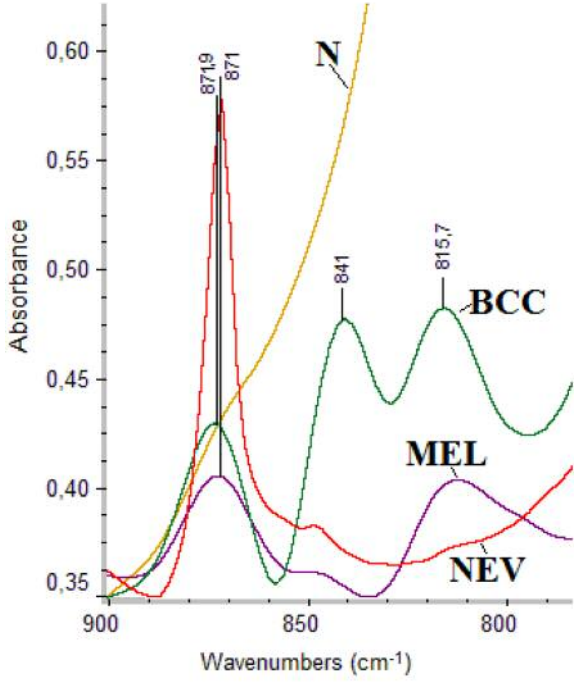

Figure 2. *FT-IR spectra of skin tissues: normal healthy tissue (N), basal cell carcinoma (BCC), melanoma (MM) and nevus (NEV), in the region 900-800 cm^{-1}.*

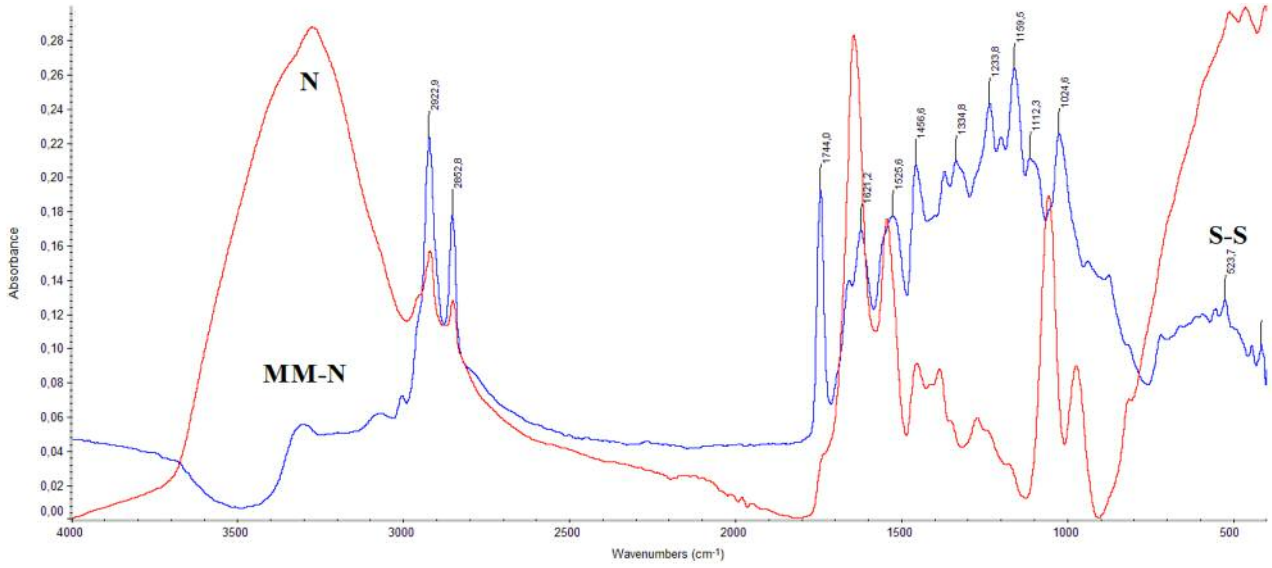

Figure 3. *FT-IR spectra of normal skin tissue (N) subtracted from the spectra of melanoma (MM) tissue (MM-N).*

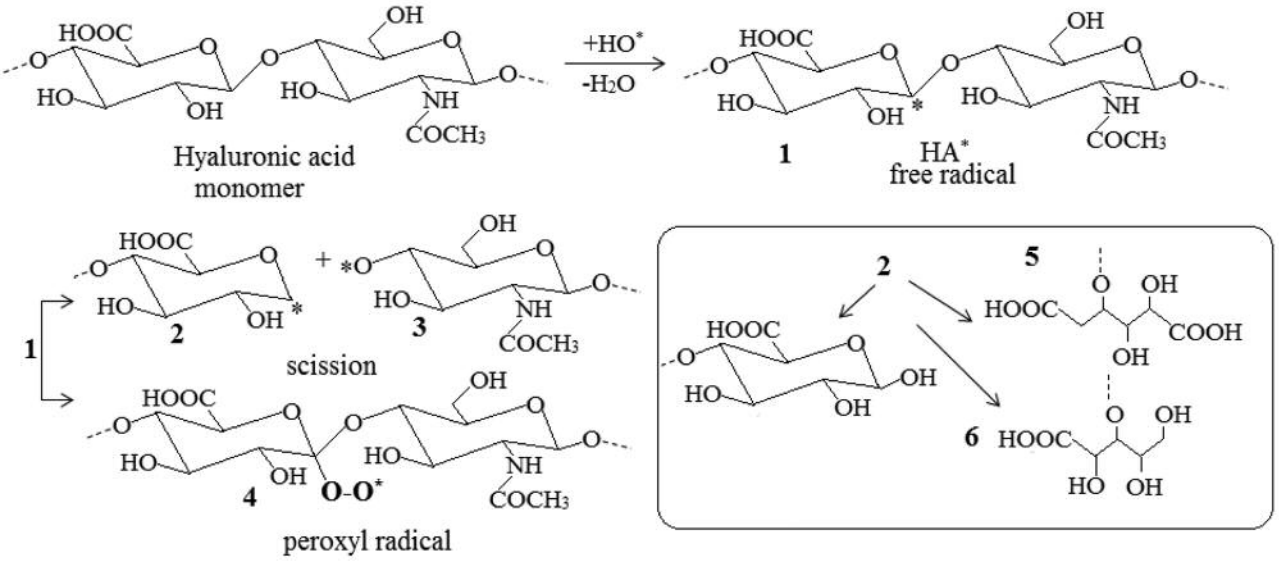

Figure 4. *Reactions of hyaluronic acid (HA) with hydroxyl free radicals (HO*). The site of HA* radical formation is random and one monomer is shown here, which is denoted by the dashed lines. The final byproducts 5 and 6 are stable and are produced from the free radical 2.*

From the above spectroscopic results it is shown that the disease affects the structure of the skin at a molecular level. In order to understand the behavior of the disease, we subtracted the spectra of the normal tissue (N) from the spectra of melanoma (MM), as it is shown in Figure 3. In the subtracted spectra of MM-N, the *v*OH and *v*NH bands are negative, suggesting the dehydration and collagen degradation of MM tissue, respectively. On the contrary, the absorption bands in the region of 1200-900 cm^{-1}, which correspond to the -C-O-C, C-OH groups, showed increased intensity. These findings lead to the suggestion that during melanoma progression the glycosylation of the tissue is

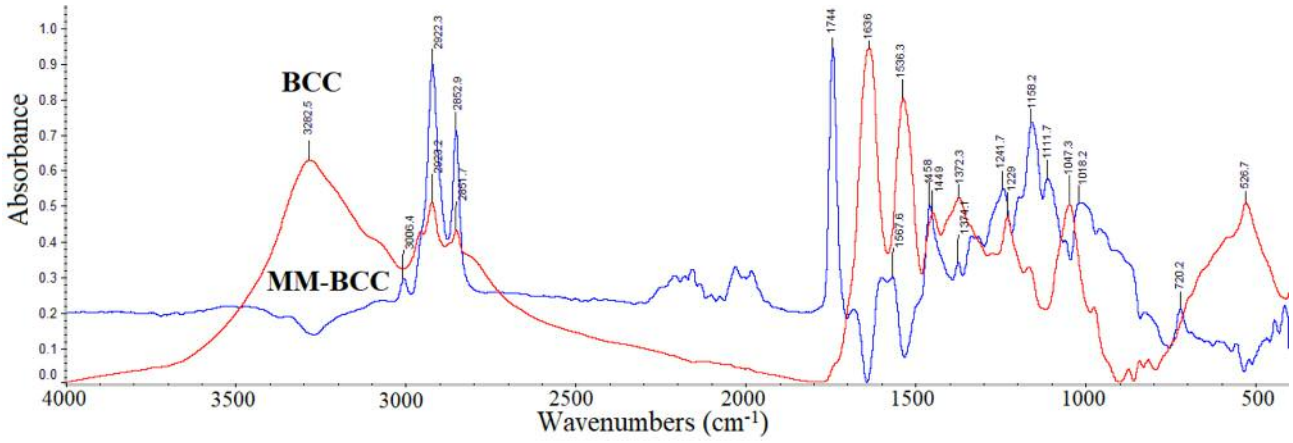

Figure 5. *FT-IR spectra of basal cell carcinoma (BCC) subtracted from the spectra of melanoma (MM) tissue (MM-BCC).*

increased. In order to explain the above spectral changes, we have to take in consideration that during melanoma development free hydroxyl radicals are produced, which play a crucial role in glycosaminoglycans fragmentation. The hydroxyl free radicals react with HA by subtracting hydrogen atoms and lead towards the formation of hyaluronic acid free radical (HA*) (Figure 4).

In Figure 4, the formed HA* free radicals (Figure 4, product 1) are not stable and are decomposed to give a series of more stable products (Figure 4, products 5 and 6) or interact with molecular oxygen to give peroxides (Figure 4, product 4). These reactions could explain the observed reduction in the intensity of the band at 1054 cm^{-1} (Figure 5, negative absorption at MM-N spectra). The produced HA* can also interact with other radicals of the cell macromolecules to produce branched or cross-linked polymers as it was detected by the band at 2892 cm^{-1}, assigned to νCH_2. The formed products are similar to those that were also produced upon irradiation of polysaccharides or by using cupric ions (Cu^{2+}) and ascorbic acid (27-29). The glycosylation has also been shown in other cancers, such as breast and metastatic bone cancers (12, 22, 30). Furthermore, HA and its CD44 cellular receptors, and the receptor for HA-mediated motility/intracellular HA-binding protein have also been linked to cancer progression and metastasis (31-34). The intensity of the bands of amide I at 1634 cm^{-1} and amide II at 1542 cm^{-1} was reduced in MM, suggesting that the proteins had a radon coil configuration and increased active sites. These sites may react with free radicals and finally lead to fragmentation of collagen chain.

The spectrum of BCC and the spectra of subtraction of BCC from MM spectrum (MM-BCC) are shown in Figure 5, in the region of 4000-2820 cm^{-1}. The 3293 cm^{-1} band of BCC assigned to νNH_2 became negative in MM-BCC, whereas the high-intensity band at 1744 cm^{-1}, which is not shown in BCC spectra or is shown as shoulder, indicated that a higher amount of aldehydes is produced in MM, due to peroxidation of lipids. This aldehydic band at 1744 cm^{-1} is observed in all cancer samples and is formed by lipid-hydroxyl free radical initiation reactions following the peroxidation of lipid radicals (18, 35). The bands of amide I at 1634 cm^{-1} and amide II at 1542 cm^{-1}, after subtraction, showed negative absorptions for MM, suggesting that in BCC more collagen is produced, in agreement with literature (36, 37). Another important difference was observed in the region 1200-900 cm^{-1}, where the bands that characterize the presence of glycosaminoglycans are found. Especially, the band at approximately 1048 cm^{-1} in MM was reduced, while in BCC was strong. This band is due to carbon-oxygen-carbon bridges (C-O-C) and is assigned to C-O vibrations of HA. The absorption at 1048 cm^{-1} could be used as a "marker band" of MM, and due to the presence of many HA-chain breaks it might discriminate melanoma from non-melanoma cancers. In the DNA region (Figure 2), only the Z-DNA form is detected in MM, while in BCC both B-DNA and Z-DNA are present in the spectra of the skin.

The increase of absorption band intensities of methyl and methylene groups of alkyl chains might be attributed to the fact that the environment becomes more lipophilic, as a result of lipid peroxidation, aldehyde and amyloid protein formation (10-12, 19). This lipophilic environment changes the permeability of cell membranes, leading to inactivation of the skin's defense systems. It has been previously shown (2) that, in skin cancers, the concentrations of the lipophilic antioxidants a-tocopherol, β-carotene, and ubiquinol-10, is much higher than in the normal skin. This fact may suggest

that the lipophilic environment dissolves these antioxidants and thus, the skin is not any more protected.

Conclusion

The high-quality recorded spectra of non-pretreated skin biopsies may be used to differentiate the types of skin cancers and further understand the biochemical processes that take place in cancer regions. The IR spectra of the skin cancers, BCC, MM, and NEV, all showed the new band at 1744 cm^{-1}. This band indicates that in cancer regions free radicals (ROS) are produced, leading to lipid peroxidation (11, 12) and subsequently to aldehydes (-CHO). The present spectroscopic data showed that melanoma changes the permeability of the cell membrane and it also alters the native B-DNA form into Z-DNA form. Characteristic IR absorption bands or "signature bands" at 841 cm^{-1} and 815 cm^{-1} have been found and are assigned to the above B-DNA and Z-DNA, respectively. It was found also that glycosylation occured more frequently in MM than in BCC and NEV. Moreover, the absorption band at 1048 cm^{-1} may also be used as a "marker band" for the presence of MM and also for HA chain fragmentation.

Acknowledgements

M. K. thanks Siemens for the financial support (contract No: 2016-017-0173-1794.M, IKY Fellowships of Excellence for Postgraduate Studies Greece Siemens Program).

References

1 Seebode C, Lehmann J and Emmert S: Photocarcinogenesis and skin cancer prevention strategies. Anticancer Res *33(3)*: 1371-1378, 2016.

2 Grammenandi K, Kyriazi M, Katsarou-Katsari A, Papadopoulos O, Anastassopoulou I, Papaioannou GT, Sagriotis A, Rallis M and Maibach HI: Low-molecular-weight hydrophilic and lipophilic antioxidants in nonmelanoma skin carcinomas and adjacent normal-looking skin. Skin Pharmacol Physiol *29*: 324-333, 2016.

3 Delinasios G: UVA-induced oxidative stress and DNA damage in human skin cells and photoprotection by antioxidant compounds. PhD Thesis, King's College, London, UK, 2012.

4 Fell Gl, Robinson KC, Mao J, Woolf CL and Fisher DE: Skin β-endorphin mediates addiction to UV light. Cell *157(7)*: 1527-1534, 2014.

5 Brauche E, Johannsen H, Nolag S, Trude S and Schenke-Layland: Design and analysis of a squamous cell carcinoma *in vitro* model system. Biomaterials *34*: 7401-7407, 2014.

6 Chollet A, Hohl D and Perrier P: Risk of coutaneous squamous cell carcinomas: the role of clinical and pathological reports. Rep Rev Med Suisse *8(335)*: 743-746, 2012.

7 Samarasinghe Vand Madan V: Nonomelanoma skin cancer. J Cutan Surg *5(1)*: 3-10, 2012.

8 Crowson AN: Basal cell carcinoma: biology, morphology and clinical implications. Mod Pathol *19*: 5127-5147, 2006.

9 Lyng FM, Ramos IRM, Ibrahim O and Byrne HJ: Vibrational microspectroscopy for cancer screening. Appl Sci *5*: 23-35, 2015.

10 Anastassopoulou J, Boukaki E, Conti C, Ferraris P, Giorgini E, Rubini C, Sabbatini S, Theophanides T and Tosi G: Microimaging FT-IR spectroscopy on pathological breast tissues. Vib Spectrosc *51*: 270-275, 2009.

11 Anastassopoulou J, Kyriakidou M, Kyriazis S, Dritsa V and Kormas T: Protein folding and cancer. Anticancer Res *34(10)*: 5806-5709, 2014.

12 Kyriakidou M, Mavrogenis AF, Kyriazis S, Markouizou A, Theophanides T and Anastassopoulou J: An FT-IR spectral analysis of the effects of γ-radiation on normal and cancerous cartilage. In Vivo *30(5)*: 599-604, 2016.

13 Brancaleon L, Bamberg MP, Sakamaki T and Kollias N: Attenuated total reflation-Fourier transform infrared spectroscopy as a possible method to investigate biophysical parameters of stratum corneum *in vivo*. J Invest Dermatol *116*: 380-386, 2001.

14 Dritsa V, Pissaridi K, Koutoulakis E, Mamarelis I, Kotoulas C and Anastassopoulou J: An Infrared spectroscopic study of aortic valve. A possible mechanism of calcification and the role of magnesium salts. In Vivo *84*: 91-98, 2014.

15 Theophanides T: Food quality and medical applications. InTech, Europa, www.Intechopen.com, 2014.

16 Kotoulas C, Mamarelis I, Koutoulakis E, Kyriakidou M, Mamareli V, Tanis O, Malesiou E, Theophanides T and Anastassopoulou J: The influence of diabetes on atherosclerosis and amyloid fibril formation of coronary arteries. A FT-IR spectroscopic study. Hell J Atheroscler *8*: 15-29, 2017.

17 Anastassopoulou J, Kyriakidou M, Kyriazis S, Kormas T, Mavrogenis AF, Dritsa V, Kolovou P and Theophanides T: An FT-IR spectroscopic study of metastatic cancerous bone. *In*: infrared spectroscopy-anharmonicity of biomolecules, crosslinking of biopolymers, food quality and medical applications. Theophanides T (ed.). InTech, Europa, www.Intechopen.com, Chapt 5, pp. 89-100, 2015.

18 Barth A and Zscherp C: What vibrations tell us about proteins. Q Rev Biophys *35(4)*: 369-430, 2002.

19 Mavrogenis A, Kyriakidou M, Kyriazis S and Anastassopoulou J: Fourier transform infrared spectroscopic studies of radiation therapy induced molecular changes in bone and cartilage. Expert Rev Qual Life Cancer Care *1(6)*: 459-469, 2016.

20 Theophanides T: Fourier transform infrared spectra of calf thymus DNA and its reactions with anticancer drug cis-platin. Appl Spectrosc *35*: 461-465, 1981.

21 Wood BR: The importance of hydration and DNA conformation in interpreting infrared spectra of cells and tissues. Chem Soc Rev *45(7)*: 1980-1998, 2015.

22 Conti C, Ferraris P, Giorgini E, Rubini C, Sabbatini S, Tosi G, Anastassopoulou J, Arapantoni P, Boukaki E, Theophanides T and Valavanis C: FT-IR Microimaging Spectroscopy: Discrimination between healthy and neoplastic human colon tissues. Mol Struc *881*: 46-51, 2008.

23 Theophanides T and Tajmir-Riahi HA: Flexibility of DNA and RNA upon binding to different metal cations. An Investigation of the B to A to Z conformational transition by Fourier transform infrared spectroscopy. J Biomol Struct Dyn *2*: 995-1004, 1985.

24 Theophanides T and Tajmir-Riahi HA: FT-IR spectroscopic evidence of C2'-endo, anti, C3'-endo, anti sugar ring pucker in 5'-GMP and 5'-IMP nucleotides and their metal-adducts. *In*: Structure and motion: Membrane, Nucleic Acids & Proteins.

Clementi E, Gorongiu G, Sarma MH, Sarma RH (Eds.). ISBN Adenine Press, New York. pp. 521-530, 1985.
25 El-Naggar NE and El-Ewasy SM: Bioproduction, characterization, anticancer and antioxidant activities of extracellular melanin pigment produced by newly isolated microbial cell factories *Streptomyces glaucescens* NEAE-H. Sci Rep *7*: 42129, 2017.
26 Riesz J: The spectroscopic properties of melanin. Thesis, University of Queensland, Queensland, Australia, 2007.
27 Choi J-I, Kim J-K, Kim J-H, Kweon D-K and Lee J-W: Degradation of hyaluronic acid powder by electron beam irradiation, gamma ray irradiation, microwave irradiation and thermal treatment: A comparative study carbohydrate polymers. Carbohydr Polym *79*: 1080-1085, 2010.
28 Valachova K, Hrabarova E, Priesolova E, Nagy M, Baňasová M, Juránek I and Šoltes L: Free-radical degradation of high-molecular-weight hyaluronan induced by ascorbate plus cupric ions. Testing of bucillamine and its SA981-metabolite as antioxidants. J Pharm Biomed Anal *56*: 664-670, 2011.
29 Shah A, Masoodi FA, Gani A and Ashwar BA: Effect of γ-irradiation on antioxidant and anti-proliferative properties of oat β-glucan. Radiat Phys Chem *117*: 120-127, 2015.
30 Varelas X, Bouchie MP and Kukuruzinska MA: Protein N-glycosylation in oral cancer: Dysregulated cellular networks among DPAGT1, E-cadherin adhesion and canonical Wnt signaling. Glycobiology *24(7)*: 579-591, 2014.
31 Ahrens T, Assmann V, Fieber C Termeer CC, Herrlich, Hofmann M and Simon JS: CD44 is the principal mediator of hyaluronic-acid-induced melanoma cell proliferation. J Invest Dermatol *116(1)*: 93-101, 2001.
32 Adamia S, Pilarski PM, Belch AR and Pilarski LM: Aberrant splicing, hyaluronan synthases and intracellular hyaluronan as drivers of oncogenesis and potential drug targets. Curr Cancer Drug Targets 13: 347-361, 2013.
33 Zhang L, Underhill CB and Chen L: Hyaluronan on the surface of tumor cells is correlated with metastatic behavior. Cancer Res *55(2)*: 428-433, 1997.
34 Goebeler M, Kaufmann D, Bröcker E-B and Klein CE: Migration of highly aggressive melanoma cells on hyaluronic acid is associated with functional changes, increased turnover and shedding of CD44 receptors. J Cell Sci *109*: 1957-1964, 1996.
35 Marmett IJ: Lipid peroxidation-DNA damage by malondialdehyde. Mutat Res *424*: 83-95, 1999.
36 Jones JC, Steinman HK and Goldsmith BA: Hemidesmospmes, collagem VII, and intermediate in basal cell carcinoma. J Invest Dermatol 98(5): 662-671, 1989.
37 Tanjore H and Kalluri R: The role of type IV collagen and basement membranes in cancer progression and metastasis. Am J Pathol *168(3)*: 715-717, 2006.

Received August 28, 2017
Revised October 14, 2017
Accepted October 23, 2017